# Small-Angle Neutron Scattering Studies of Low-Polarity Telechelic Ionomer Solutions. 1. Total Scattering

**Eleni Karayianni, Robert Jérôme,† and Stuart L. Cooper*,‡**

*Department of Chemical Engineering, University of Wisconsin—Madison, 1415 Johnson Drive, Madison, Wisconsin 53706*

*Received January 10, 1995; Revised Manuscript Received May 21, 1995*®

ABSTRACT: The overall structure and thermodynamic interactions that take place in low-polarity ionomer solutions have been investigated via the technique of small-angle neutron scattering for two Na-neutralized carboxy-telechelic polystyrene model ionomer systems that differ in the length of the polymer backbone. The strong interchain association that is evidenced in the viscometric measurements of the ionomers compared to the ester forms is apparent in the scattering profiles of the ionomers that show a characteristic upturn that extends in the low-$q$ regime and increases with increasing polymer concentration. The apparent molecular weight and size of the aggregated particles show a significant increase over a small concentration range, while the ionic content seems to not affect the degree of association in the concentration regime studied. The supramolecular structure of the ionomer solutions is revealed by fitting the scattering data to a scaling law in the intermediate $qR_g$ regime that supports a percolation type of behavior for the ionomer clusters for both systems studied. The fractal dimension of the aggregates is 1.76 for both ionomer systems which provides evidence for a rather extended configuration and high polydispersity of the clusters in solution. The molecular weight of the associating particles is observed to rapidly approach infinity with increasing polymer concentration, indicating the approach to a gel transition. The scattering data of the ionomer solutions were fitted to the de Gennes model based on the random-phase approximation theory. The Flory−Huggins interaction parameter of the ionomer solutions determined using this model shows a strong concentration dependence with a quite unexpected increase with decreasing polymer concentration. The thermodynamic interactions in the ionomer solutions were changed dramatically by the association as revealed by a significant decrease of the second virial coefficient.

## I. Introduction

Ionomers are polymers that have a small amount (usually less than 10 mol %) of ionic groups covalently bonded to the polymeric backbone. After more than 20 years of research on ionomers there are still unanswered questions about the structural characteristics and morphology of these materials that lead to their unique properties. This is mainly due to the ionic interactions that add to the complexity of the material behavior. Up to now, most research on ionomers has been focused on their solid-state behavior. In the bulk, it is generally accepted that the unusual behavior of ionomers originates from ionic group interactions that lead to aggregation of ions into microdomains, which act as physical cross-links in the material.[1] However, the morphological features induced by the microphase separation that involve the shape, distribution, and arrangement in space of the ionic microdomains are still a subject of controversy.[2] Compared to the extensive investigation that has been conducted in the bulk, the solution behavior of ionomers has been relatively less explored despite the unique properties observed in this area as well.[3] In solution, the unusual behavior exhibited by ionomers originates from the fact that the ionic interactions can be altered by controlling the environment surrounding the ionic groups. An intriguing area of ionomer solution research has involved the study of mainly nonpolar hydrocarbon-based ionomer chains in low-polarity solvents. These solutions have been shown to exhibit behavior similar to that in bulk: the low-polarity environment of the solvent favors strong dipolar interactions between ion pairs that result in intermolecular association. Evidence of association in low-polarity ionomer solutions has been most dramatically demonstrated by a significant enhancement of the viscosity of the ionomer solution compared to its nonionic analog. The most significant feature of this phenomenon is that it occurs at low polymer concentrations.

Solution studies of ionomers have mostly focused on random copolymer ionomer systems that have the ionic groups randomly placed along the polymeric backbone. The solution properties of these systems have been observed to strongly depend on concentration. Viscometric measurements of low-polarity random ionomer solutions have detected the existence of a crossover concentration, $c^*$.[3−6] Below $c^*$, the ionomer solution viscosity is reduced compared to the nonionic parent polymer. Above $c^*$, a significant increase of the ionomer viscosity is observed over that of the parent polymer that is further enhanced as polymer concentration or ion content increases. This enhancement in the ionomer solution viscosity is considered to arise from intermolecular interactions which increase the apparent molecular weight and hence the viscosity and lead to the formation of multimers, particles that consist of many polymer chains interconnected through the ionic dipoles. In the low-concentration regime the reduced intrinsic viscosity of the ionomer solution compared to its nonionic analog was originally attributed to intramolecular interactions which lead to single-chain collapse.

Light and small-angle neutron scattering (SANS) have been applied to structural investigations of random copolymer ionomer solutions responsible for the observed viscometric behavior. Scattering experiments on

* Author to whom correspondence should be sent.
† Center for Education and Research on Macromolecules (CERM), University of Liège, Sart-Tilman, B6 4000 Liège, Belgium.
‡ Current address: College of Engineering, University of Delaware, 135 Dupont Hall, Newark, DE 19716.
® Abstract published in *Advance ACS Abstracts,* August 15, 1995.

0024-9297/95/2228-6494$09.00/0 

low-polarity solutions of randomly sulfonated polystyrene ionomers (SPS) have shown that the average weight and size of the scattering particles increase with concentration, supporting multimer formation. However, interchain association was shown to persist even at concentrations below $c^*$.[7,8] In addition, single-chain scattering studies showed that the single-chain dimensions were not affected by association in the semidilute concentration regime for the different ionic levels studied.[8-10] This suggests that the interpretation of the viscometric results, which involved a transition from intramolecular to intermolecular interactions around the crossover concentration, is incorrect.[11,12] A recent dynamic light scattering study of SPS in xylene has reported the existence of a crossover concentration that corresponds to the transition between single-chain dynamics and multichain aggregate dynamics. This transition is, however, almost 10 times lower than the $c^*$ detected in the viscometric experiments.[13] Therefore, interpretation of the actual structure of ionomer solutions has to take into account the sensitivity of each experimental technique to probe different moments of the particle distribution in solution.

Due to the non-well-defined architecture of the random copolymer ionomers, structural studies on these systems are restricted in providing the overall characteristics of the association phenomenon. Halato-telechelic ionomers that have the ionic groups fixed at the ends of the polymeric backbone have proved to be a very attractive system for exploring ionomer solution properties. Telechelic ionomers have shown the same general behavior as the random copolymer ionomer systems; therefore, they can be used as a model system to provide the correlations that define the behavior of ionomers in general.[14] Solution studies of these systems have, however, been mostly explored through viscometric investigations only.[15-18] In low-polarity solvents a significant enhancement of the ionomer viscosity is observed, in analogy to the random copolymer ionomers. However, the increase in viscosity that is observed in telechelic ionomer solutions with increasing polymer concentration is much sharper and eventually leads to gelation at very low concentrations (1-2 g/dL).[15,17] Such an abrupt gelation transition has not been observed in the random copolymer ionomer solutions in which the viscosity slowly increases with concentration. In telechelic ionomer solutions the observation of a crossover concentration, $c^*$, in the viscometric curves, analogous to the random ionomer solutions, has not been reported in the majority of studies in this area. A crossover concentration has, however, been observed in highly dilute solutions of quaternary ammonium-telechelic polystyrene ionomers[19] which is an indication that a $c^*$ may also be apparent in model telechelic ionomer solutions at lower concentrations. This behavior should be compared to a decrease of the crossover concentration that has been observed to take place in random copolymer ionomer solutions as the polymer molecular weight decreases.[20] Although such a behavior was originally interpreted in terms of the smaller number of ionic groups per polymer chain in telechelics compared to the random copolymer ionomers which makes intramolecular association less favorable,[20] intramolecular association in telechelic ionomer solutions has been supported by viscometric,[19] fluorescence,[21] and SANS measurements.[22] The gelation concentration has been observed to be strongly dependent on the polymer molecular weight, decreasing with increasing molecular weight.[23,24]

In low-polarity ionomer solutions it might be expected that the structure in solution is related to the morphological features that have been associated with the bulk morphology of ionomers. However, investigations on the internal structure of the ionomer aggregates as well as structural studies of model ionomer systems in solution are limited.[22,25,26] A recent small-angle X-ray scattering (SAXS) study on concentrated low-polarity solutions of halato-telechelic ionomers has observed no structural discontinuity from the bulk to the solution state.[27] Upon dilution the interaggregate distance increases, while the average number of chains per multiplet remains constant. Further dilution results in partial aggregate dissociation, while the interaggregate distance remains constant. In this paper we shall attempt to probe the structural characteristics that are responsible for the association phenomenon observed in ionomer solutions by studying a model telechelic ionomer system. This paper reports the results of small-angle neutron scattering (SANS) experiments from the multimers in the dilute concentration regime. To this end, SANS is a unique tool to probe the structure of the associating particles, as coverage of a wide $q$ range can allow for determination of the statistics and scaling laws that govern the association phenomenon. In order to utilize the whole experimental range attainable from the SANS experiment, a molecular model is required that describes the interparticle scattering function. In this study the de Gennes model that has been widely applied in the polymer solution literature is considered. The application of this model to the ionomer solutions allows for an indirect determination of the single-chain dimensions as well as the thermodynamic Flory-Huggins interaction parameter, $\chi_{PS}$, of the ionomer solutions. Based on the experimental findings, the structure and thermodynamics of the ionomer solutions are analyzed according to techniques that have been developed for associating solutions and a possible structure for the aggregated chains is suggested.

## II. Experimental Section

**A. Synthesis of Telechelics.** The materials that are reported in this study are halato carboxy-telechelic polystyrene ionomers neutralized with sodium. These materials belong to the larger group of carboxylato-telechelic ionomers that have been synthesized and studied by the group of R. Jérôme at the University of Liège, Liège, Belgium.[28] The materials have been synthesized according to the synthetic procedures reported by Broze et al.[15] and Jérôme.[28] Carboxylic acid-telechelic polystyrenes were synthesized by anionic polymerization of styrene (99%, Aldrich) to produce a narrow molecular weight distribution. Naphthyllithium was used as a difunctional initiator that produces chains with exclusively styrene units.[21] Carbon dioxide was used as the deactivating agent to end-cap polystyrene chains with a carboxylic acid group, which was either quantitatively neutralized with sodium methoxide with formation of the ionomer or quantitatively esterified with diazomethane[29] to produce the nonionic analog. The functionality of the ionomers is better than 1.95 as determined from potentiometric titration of the acid end groups in a 90/10 (v/v) toluene/methanol mixture using tetramethylammonium hydroxide.

**B. Molecular Weight Characterization.** The molecular weights of the polymers were characterized in the ester forms, that are expected to lack ionic association, using gel permeation chromatography (GPC), intrinsic viscometry (IV), and static light scattering (SLS) techniques.

**1. GPC Measurements.** GPC was performed on a Waters 501 apparatus with two Ultrastyragel columns, in dimethylacetamide (DMA) at 50 °C, 1 mL/min, at 0.1 g/dL polymer concentration, using both refractive index (RI) and ultraviolet

**Table 1. Moments of the Molecular Weight Distribution of the Hydrogenated Telechelic Esters Evaluated from GPC Experiments**

| material | GPC results $M_n$ | $M_w$ | $M_z$ |
|---|---|---|---|
| e−6 | 7780 | 8500 | 9220 |
| e−17 | 17800 | 19120 | 20310 |

(UV) detection at 266 nm. Polystyrene standards of low molecular weights from 2000 to 50 000 were used for the determination of the GPC calibration curve. The number-, weight-, and $z$-average molecular weights of the hydrogenated telechelic esters calculated from the GPC measurements are shown in Table 1. The nomenclature that will be used throughout this study will be symbolized as $m-x$ where $m$ denotes the form of the material which is e for the ester and i for the ionomer and $x$ denotes the targeted prepolymer molecular weight in thousands. The polydispersity is less than 1.10 for all materials.

**2. Viscometry Measurements.** Intrinsic viscosity measurements were performed on an AVS 300 Schott-Geräte semiautomated viscometer measuring station for dilution sequences using KPG-Ubbelohde capillary viscometers placed in a measuring stand. Temperature control was achieved to within 0.05 °C or better using a transparent thermostated bath. The flow times of the solutions were in all cases larger than 200 s, and the Hagenbach correction was applied for the specific capillary used. The correction in no case exceeded the error tolerance of the time measurement. Special care was given to the cleaning of the viscometers, as viscosity measurements are very sensitive to the cleaning procedure. After rinsing with the solvent, the capillary viscometer was left in nochromix solution overnight, followed by rinsing with water and acetone, and then allowed to dry in an oven for about 8 h. The solutions were filtered with a Millex-LCR 0.5 $\mu$m pore size filter from Millipore Co. and left for ~30 min in the thermostated bath prior to measurements to achieve temperature equilibration and homogeneity after dilution. The highest concentration for each sample was determined by weighing the sample in a high-precision balance and then dissolving in a specific amount of solvent. The lower concentrations were determined by dilution with a precise amount of solvent. All solutions were prepared in anhydrous toluene (99.8%, Aldrich). The viscosities that are reported in this paper are with respect to kinematic viscosity values.

For each material the reduced viscosity of an average of eight different concentrations, in the range 0.3−2.0 g/dL, was determined. The overlap concentration based on viscometric measurements, $c^*_v$, is usually considered to be $c^*_v = 2.5/[\eta]$,[30,31] where $[\eta]$ is the intrinsic viscosity of the polymer solution. In all cases, $c^*_v$ was more than 10 times larger than the highest concentration studied. In addition, the specific viscosity of the polymer solutions was less than 0.6 which verifies that the concentration regime studied is well within the dilute solution limit. In the dilute concentration regime where $[\eta]c \ll 1$, the reduced viscosity of nonionic polymer solutions is linear with concentration and can be described by the Huggins equation:

$$\eta_{sp}/c = [\eta] + k_1[\eta]^2 c \qquad (1)$$

where $\eta_{sp}$ is the specific viscosity of the solution, $c$ is the polymer concentration (w/v), and $k_1$ is the Huggins constant. For all the esters studied the Huggins constant was found to be larger than the value of 0.3 that this parameter usually assumes for solutions in good solvent and it varied from sample to sample. This discrepancy in $k_1$ is expected to arise from the small difference that exists between the reduced and intrinsic viscosities due to the low molecular weight of the polymers, that makes a precise evaluation of the slope of the viscometric curve very sensitive to the instrumental accuracy. The intrinsic viscosities, however, were determined with high precision.

The Mark−Houwink equation, that is the most commonly used expression to extract molecular weight information from intrinsic viscosity measurements, is only valid over a limited range of molecular weights and breaks down for low molecular weight polymers.[32] Intrinsic viscosity data from the literature for the system polystyrene/toluene suggest that the use of any relation fails around a molecular weight of 10 000. Since the polymers studied fall both below and above this value, a broad range of molecular weight standards would be needed for study along with the application of a different relation in each regime. In this study, in order to determine the correlation between the intrinsic viscosity and viscosity-average molecular weight, we have used the results of a theory developed by Han,[33] based on arguments of the blob theory, that has been shown to be an excellent description of the system polystyrene/toluene over an extremely broad molecular weight range.[34] The relations necessary for the calculations are given in eqs 2−4,

**Table 2. Molecular Characterization of the Hydrogenated Carboxy-Telechelic Polystyrene Methyl Esters in Toluene at 25 °C**

| material | $[\eta]$, dL/g | $M_v$[a] | $M_w$[b] | dn/dc | $c^*_{LS}$, g/dL | $(M_w)_{app}$[c] | $(R_g)_{app}$,[c] Å |
|---|---|---|---|---|---|---|---|
| e−6 | 0.0872 | 7120 | 9520 | 0.108 | 3.4 | 8860[1] | 32.0[1] |
| e−17 | 0.1479 | 20220 | 21880 | 0.104 | 2.1 | 23190[2] | 68.6[2] |

[a] From intrinsic viscometry measurements. [b] From light scattering measurements. [c] From SANS experiments on the esters as described in the text: (1) 1.04 and (2) 1.45 g/dL.

$$[\eta] = [\eta]_0 F(M/M_1) \quad \text{where} \quad [\eta]_0 = K_0 M^{1/2} \qquad (2)$$

$$F(M/M_1) = 1 \quad \text{for} \quad M > M_1 \qquad (3)$$

$$F\left(\frac{M}{M_1}\right) = \frac{4}{3}x^{1/2}\frac{x^{-2}\left(3-\frac{2}{x}\right)+6x^{1/5}\left[\frac{5}{11}(1-x^{-11/5})-\frac{5}{16}(1-x^{-16/5})\right]}{2\left(1-\frac{1}{3x}\right)+\frac{5}{2}(x^{2/5}-1)-\frac{5}{7}(x^{2/5}-x^{-1})} \quad \text{for} \quad M < M_1 \qquad (4)$$

in which $x \equiv M/M_1$. The fit of a number of monodisperse polystyrene samples with molecular weights from 660 to $4 \times 10^6$ in toluene at 25 °C to these equations yielded the values of the parameters: $K_0 = 0.1033$; $M_1 = 14\,000$. The validity of these equations was tested with four narrow distribution polystyrene standards of $M_w$: 5120, 9000, 12 200, and 17 500. The intrinsic viscosities and molecular weights, $M_v$, of the telechelic esters obtained from this analysis are given in Table 2. These values are in satisfactory agreement with the GPC experimental results.

**3. Static Light Scattering Measurements.** Light scattering experiments have been performed using a Malvern 4700C light scattering system operating with a 2-W $Ar^+$ laser, stabilized with etalon to provide monochromatic light at 488 nm. A quartz cylindrical cell was used as the sample cell. The refractive matching fluid used was decahydronaphthalene which was filtered through a pump filter before the measurements. The temperature of the sample was kept constant to better than 0.1 °C through external circulation of water around the sample holder. With the use of a computer-controlled goniometer the scattered intensity was measured at scattering angles from 30° to 140°. Each solution to be tested was prepared separately by dissolving a precisely weighed sample in a specific amount of spectrophotometric grade solvent. The solutions were left for 1 day for complete dissolution and filtered through a 0.2-$\mu$m Millipore filter unit prior to introducing them into the cell. The pure solvent was clarified through filtration with a 0.1-$\mu$m Millipore filter unit.

The overlap concentration for light scattering experiments, $c^*_{LS}$, is usually considered as[35] $c^*_{LS} = 1.31 \times 10^{-25} M_w/\langle R_g^2\rangle^{3/2}$, where $\langle R_g^2\rangle^{1/2}$ is the root-mean-square radius of gyration of the polymer chain. In order to obtain high enough counts and good statistics of the scattered intensity, concentrations higher than

$c^*_{LS}$ were also measured. In this regime a Zimm plot is no longer linear with concentration since the third virial coefficient of the polymer solution, $A_3$, becomes significant as well. At all concentrations studied, the dimensionless quantity $A_2M_wc$, where $A_2$ is the second virial coefficient, was less than unity, and therefore the inverse reduced intensity can be expressed as an expansion in the power series of concentration as[36]

$$\frac{Kc}{(\Delta R_\theta)_{\theta\to 0}} = \frac{1}{M_w} + 2A_2c + 3A_3c^2 + \ldots \quad (5)$$

where $K$ is the optical constant defined in this case for vertically incident polarized light as $K = (4\pi^2 n_0^2(dn/dc)^2)/(\lambda_0^4 N_A)$ where $n_0$ is the solvent refractive index, $dn/dc$ is the refractive index increment of the solution, $\lambda_0$ is the wavelength under vacuum, and $N_A$ is Avogadro's constant. $\Delta R_\theta$ is the excess Rayleigh ratio that was converted to absolute scaling through comparison of the polymer scattering to that of spectrophotometric grade toluene (99.5%, Aldrich). The Rayleigh ratio of the standard for unpolarized detected light at 25 °C and 488 nm was obtained as[37] $39.6 \times 10^{-6}$ cm$^{-1}$, and the refractive index as 1.49413.[38] The refractive index increments of the polymer solutions were measured via a KMX-16 laser differential refractometer at 633 nm using at least four concentrations in the concentration regime 0−1 g/dL. The measured values agreed within experimental error with the literature values for low molecular weight polystyrene solutions under similar experimental conditions,[39,40] and therefore the literature data reported at 488 nm for the same solutions[41,42] were considered in the calculations to take into account the wavelength dependence of $dn/dc$. The $dn/dc$ of the telechelic esters in toluene are shown in Table 2.

For each material eight different concentrations were measured. Due to the low molecular weight of the telechelics, the scattering angle dependence of the reduced intensity was very small which prevents determination of the polymer chain dimensions in solution from this experiment. $(\Delta R_\theta)_{\theta=0}$ was evaluated from a linear extrapolation of $(Kc/\Delta R_\theta)$ versus $q^2$. The weight-average molecular weights of the materials were determined by performing a nonlinear least-squares fit of eq 5[35] with fitting parameters $M_w$, $A_2$, and $A_3$. The accuracy of the results was also tested through the Bawn plot[43] that requires only $A_2$ and $A_3$ as the fitting parameters. Both methods resulted in the same values of the parameters. From these analyses the molecular weights were evaluated with an accuracy of ±10%. The sensitivity of this technique in this low-$M_w$ regime was observed to be larger in the determination of the virial coefficients so that a larger number of concentrations would be required to measure these quantities with higher accuracy.[39] The molecular weights thus determined, as well as the estimated overlap concentrations are presented in Table 2. Light scattering is observed to result in higher $M_w$'s than GPC. However, the deviation between the two techniques is less than 15% which is reasonable considering the low molecular weight of the materials and their relative determination from GPC. In the analysis that follows the polymer molecular weights that are involved in the calculations are those determined from the light scattering experiments.

**C. Small-Angle Neutron Scattering Sample Preparation and Data Acquisition.** The small-angle neutron scattering (SANS) experiments were performed on the 30-m SANS instruments at the Cold Neutron Research Facility (CNRF) at the National Institute of Standards and Technology (NIST) in Gaithersburg, MD. The scattering data were obtained during two visits at NIST in May and Nov 1992.[44] During the first visit data acquisition was performed on the SANS instrument connected to the NG-7 neutron guide. The system configuration was set at a sample−detector distance of 9 m, a neutron wavelength of 6 Å and a detector center offset of 22 cm that provided data in the $q$ range 0.0062−0.0722 Å$^{-1}$. Quartz cells of 5-mm thickness were used that were determined based on the known coherent and incoherent atomic cross sections to give sample transmissions within 0.5−0.8.[45,46] Multispecimen holders that allowed for five to seven different cells to be held inside the sample chamber were used. The temperature of the solutions was controlled electronically to ±0.1 °C. Data were acquired in time slices of 10 min. The total counting time was varied for each sample so that at least $4 \times 10^5$ and up to $7 \times 10^5$ counts were collected to achieve satisfactory statistics in the scattering data. The scattering data from each solution were corrected for the scattering from the empty cell and the background (using a $^6$Li blocked beam). The scattering from the solvent was corrected in a similar way and was subtracted from the corrected solution scattering to obtain the scattering from the polymer alone. To correct for the differences in transmission that exist between the sample and the empty cell, transmissions from the cell plus sample, empty cell, and cell plus solvent were measured. The transmission measurements were made through attenuation of the beam with the use of appropriate thickness Plexiglass and comparison of the direct beam intensity between the sample and empty beam. The subtracted data were finally corrected for the detector response, which becomes nonlinear toward the edges, by applying predetermined correction factors and masking the edges of the detector according to procedures developed at NIST for the Oak Ridge type detector of the NG-7 SANS instrument. The scattering data were then radially averaged as none of the samples exhibited anisotropy on the two-dimensional contour plot and placed on an absolute scale by measuring the scattering of a 1-mm-thickness silica gel standard that has a zero cross section of $d\Sigma/d\Omega(0) = 32 \pm 1$ cm$^{-1}$. The standard allows reduction of the two-dimensional scattering data to absolute cross section $(d\Sigma/d\Omega)_{abs}$ versus scattering momentum vector, $q$, which facilitates further analysis. During the second visit the experiments were performed on the 30-m SANS instrument that is connected to the NG-3 neutron guide at NIST. The system configuration was set at a sample−detector distance of 13 m, a neutron wavelength of 8 Å, and detector center offset of 0 cm that provided access to the $q$ range 0.0035−0.0271 Å$^{-1}$. The transmission measurements were performed by using a pencil detector and comparing the transmissions between the sample and the empty beam. The detector of this instrument is of the ILL type, and corrections for the detector response were taken into account by dividing the scattering data pixel-by-pixel by the measured isotropic scattering of water and then masking to correct for nonuniformities in the detector response. The data reduction scheme followed was the same as that for the measurements on the NG-7 instrument. The data were converted to absolute scaling through comparison with the scattering from a 1.5-mm partially labeled polystyrene standard C1 that has a zero cross section of $d\Sigma/d\Omega(0) = 594$ cm$^{-1}$ ± 5% and a 1-mm standard silica gel. The zero intensity of the polymer standard was evaluated according to the random-phase approximation (RPA) theory whose program is available at NIST. For the absolute scaling evaluation the transmissions of the standards were also measured at the specific wavelength of the experiments.

In order to detect the scattering from the multimers, solutions of totally hydrogenated ionomers in deuterated toluene (99+ atom % D, $d_8$, Sigma/Aldrich) were prepared. The solutions were left stirring for 5 days before the measurements to ensure homogeneity and equilibrium. In this case the coherent scattering cross section $(d\Sigma/d\Omega)_{coh}$ is[46,47]

$$\left(\frac{d\Sigma}{d\Omega}\right)_{coh} = (b_1^* - b_0^*)^2 S_{11}(q) = K_1^{*2} S_{11}(q) \quad (6)$$

where $b_1^*$ and $b_0^*$ are the total coherent scattering length densities of the monomer and solvent molecules respectively, $K_1^*$ ($\equiv b_1^* - b_0^*$) is the contrast factor between the polymer (1) and the solvent (0) based on the scattering length densities, and $S_{11}(q)$ is the polymer−polymer scattering function. $S_{11}(q)$ contains the contributions of both intra- and intermolecular scattering as follows:

$$S_{11}(q) \equiv N_1 Z_1^2 S_t(q) \quad (7)$$

$$S_t(q) = S_s(q) + S_p(q) \quad (8)$$

where $N_1$ is the number density of polymer chains, $Z_1$ is the

**Table 3. Atomic Scattering Lengths and Density of Hydrogenated Polystyrene and Deuterated Toluene**

| material | $b$, $10^{-12}$ cm [36] | $\varrho$, g/cm$^3$ | $\sigma_{inc}$, $10^{-24}$ cm$^2$ [c] | $V_i$, cm$^3$/mol |
|---|---|---|---|---|
| h-polystyrene | 2.32672 | 1.087[a] | 840.08 | 95.8 |
| d-toluene | 9.99308 | 0.9385[b] | 57.67 | 106.8 |

[a] From ref 46. [b] From ref 47. [c] The atomic incoherent scattering cross sections were obtained from ref 43 and 48 for $^1$H and from ref 48 for $^{13}$C and $^2$H. These were calculated by considering the molecular weight of the polymer repeat unit and solvent molecules to be respectively $m_0 = 104.15$ and $M_s = 100.19$.

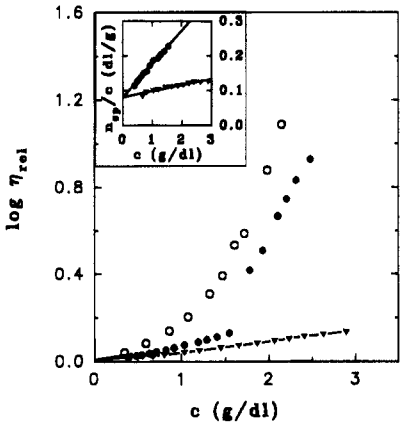


**Figure 1.** Concentration dependence of the relative viscosity of Na-neutralized carboxy-telechelic polystyrene ionomers (●) i-6 and (○) i-17 in toluene at 25 °C. For comparison the corresponding methyl ester form (▼) e-6 is also shown. In the inset of the figure the reduced viscosity versus concentration is shown for the i-6 ionomer and its ester in the lowest concentration regime studied, where both are linear with concentration.

degree of polymerization, and $S_t(q)$, $S_s(q)$, and $S_p(q)$ are the total, single-chain, and intermolecular scattering functions, respectively.

The scattering obtained after the data reduction includes both the coherent and incoherent scattering. At a reactor source where the neutron wavelength is constant, the incoherent scattering is isotropic and is therefore constant over the whole $q$ range. Because of the low polymer concentrations studied, the $^1$H content is not substantial and therefore the incoherent scattering is expected to be very small for these solutions. We have, however, compensated for the incoherent scattering from the telechelic solutions by adding a constant factor in the expression describing the coherent scattering in our modeling analysis and having this factor as an adjustable parameter during the modeling. The atomic scattering lengths and densities of the polymer and solvent molecules are presented in Table 3. The ratio of the coherent to incoherent scattering for all samples tested was larger than 10:1 at zero $q$.[51]

## III. Data Evaluation and Analysis

**A. Viscometry.** The concentration dependence of the relative viscosity of the telechelic ionomers is shown in Figure 1. For comparison, the corresponding viscometric behavior of the ester e-6 is also shown. Due to the extensive viscometric investigations that have been performed in ionomer solutions,[14,15] this experiment can be used to show that the ionomer systems studied display ionic association. Indeed, as shown in Figure 1 at low concentrations the viscosity of the ionomer is increased compared to the viscosity of the corresponding ester form, while at higher concentrations an abrupt increase of the ionomer viscosity is observed which most interestingly takes place at relatively low concentrations. This strong enhancement in viscosity is related to the gelation transition that has been observed to be unique to model telechelic ionomer solutions compared to the random copolymer ionomers. The association phenomenon is expected to increase with increasing polymer concentration, as evidenced by the increase in solution viscosity.

The observed viscometric behavior shows the same general characteristics that have been exhibited by other low-polarity carboxylato-telechelic ionomer solutions. In the low-concentration regime, that is shown in the inset of Figure 1, the intrinsic viscosities of the telechelic ionomers are observed to be the same as those of the ester forms showing the absence of a crossover concentration that has been detected in random copolymer ionomer solutions, in the concentration regime studied. The Huggins constant is observed to increase almost 5 times for the i-6 ionomer and 7 times for the i-17 ionomer compared to their corresponding ester forms. Such an increase in the initial slope of the viscosity–concentration curve has been observed in other ionomer systems as well and is considered to be indicative of association in solution.[52–54] At the same polymer concentration, the solution viscosity is enhanced for the lower ionic content ionomer, a behavior that is quite different from random copolymer ionomer solutions in which the ionomer viscosity increases with increasing ionic content.[4] This difference should be viewed in terms of the direct relation that exists between the polymer molecular weight and ionic content in telechelic ionomers that are inversely proportional to each other. In contrast, the ionic content may be varied with a fixed polymer backbone length in a random copolymer ionomer system.

**B. Modeling SANS Results.** Up to now analyses of the results obtained from the application of scattering techniques to elucidate structural information in ionomer solutions have been constrained to the low scattering vector regime. In this regime, except when short polymer molecules are considered, the molecular information extracted from a SANS experiment is equivalent to that of a more conveniently measured static light scattering experiment.[55] However, probing a wide $q$ range provides a wealth of information on the structure of the solution over a wide range of length scales. This is especially true in the case of associating systems in which both single-chain and multichain characteristics are involved. In order to describe the SANS scattering data, a model that describes the polymer–polymer scattering function has to be applied, as is apparent from eq 6. Following the random-phase approximation theory (RPA) developed by de Gennes[56] and generalized by Boué et al.,[57] the total scattering from a polymer solution of monodisperse hydrogenated polymer chains in a deuterated solvent can be written as:

$$\frac{(b_1^* - b_0^*)^2}{N_A(d\Sigma/d\Omega)_{coh}} = \frac{K_N}{(d\Sigma/d\Omega)_{coh}} = \frac{1}{Z_1\phi_1V_1S_s(q)} + \frac{1}{\phi_0V_0} - \frac{2\chi_{PS}}{v_0} \quad (9)$$

where $K_N$ is defined from eq 9, $\phi_1$ and $\phi_0$ are the volume fractions of the polymer and solvent, respectively, $V_1$ and $V_0$ are the partial molar volumes of the polymer repeat unit and the solvent molecules, respectively, $\chi_{PS}$ is the Flory–Huggins (FH) polymer–solvent interaction parameter, and $v_0$ is the lattice cell volume defined as $v_0 \equiv (V_1V_0)^{1/2}$. Evaluation of eq 9 as a model for the interparticle scattering function shows that it is the final

result of many different theoretical approaches,[58-60] and it has been theoretically proven to hold from zero concentration to the bulk.[61]

In order to utilize the whole experimental $q$ regime, the exact expression of the single-chain scattering function needs to be employed in eq 9. The discussion of the effect of the ionic association on the single-chain conformation in the telechelic ionomer solutions is presented in the following paper of this series.[62] In this paper the single-chain structure factor, $S_s(q)$, was described by applying both the Debye function, which successfully describes the scattering function of high molecular weight polymer chains,[60,63] and a wormlike chain model[64] that takes into account the short-chain nature of the telechelics. The SANS results were modeled by applying a nonlinear least-squares optimization program using the E04HEF optimization routine of the NAG Fortran library. The objective function for minimization was considered to be the sum of the squares of the residuals of the total scattering intensity. For this analysis the first and second derivatives of the objective function with respect to the fitting parameters required were analytically evaluated so that computational errors were minimized. The fitting parameters during the optimization were the incoherent scattering, $(d\Sigma/d\Omega)_{inc}$, the contrast factor $K$, and the statistical segment length $\alpha$. Inserting $K$ as a model parameter compensates for nonuniformities arising from the absolute scaling of the data. Monitoring $\alpha$ through this analysis results in information on the single-chain dimensions and conformation. The results of this analysis are presented in the following publication[62] where they are compared with the results obtained from direct single-chain SANS scattering measurements. As is shown in that report, the de Gennes model predictions agree very well with the direct measurements of the single-chain dimensions. Since the direct probe of single chains in associating systems requires experimental procedures and tools that are difficult to apply, this result is very important as probing of single chains can then be successfully determined by measurements on the more experimentally accessible total particles.

The Flory–Huggins polymer–solvent interaction parameter, although nowadays considered more as a phenomenological parameter,[65] remains a significant thermodynamic parameter in the field of polymer science. In polymer solutions this parameter is directly associated with the second virial coefficient of the solution, and it is used as a criterion to determine the thermodynamic state of a polymer–solvent system. The FH interaction parameter for polystyrene/toluene solutions has been well documented, and its value could be used in the de Gennes model for modeling the multimer scattering data. However, the presence of ionic association in the ionomer solutions is expected to have a strong effect on the intersegmental interactions in solution that are described by $\chi$. The use of SANS data to determine the FH interaction parameter is very common especially in the literature of polymer blends.[66] $\chi$ is obtained from such data in a binary mixture from the application of the de Gennes model at zero scattering angle where $S_s(q)_{q=0} = 1$. In modeling the SANS data of the ionomer solutions, we have followed a similar approach. Initially, $\chi$ was evaluated from the calculated value of $K$ from literature data and from the value of $(d\Sigma/d\Omega)_{q=0}$ obtained from the intercept of a linear plot of the experimental $(d\Sigma/d\Omega)^{-1}(q)$ versus $q^2$ at low $q$. The value of $\chi$ was then corrected for the optimized values of $K$ and $(d\Sigma/d\Omega)_{q=0}$, taking into account the best value of incoherent scattering obtained from the optimization program until convergence. The contrast factor $K$ values obtained from this minimization procedure are shown in Table 4. These values are in good agreement with the expected theoretical value of this parameter, $2.894 \times 10^{-3}$ mol/cm$^4$. Due to this good agreement in the determination of $K$, the minimization program was also tested by inserting $\chi$ as a fitting parameter while considering $K$ constant. This analysis resulted in the same values for $\chi$ as the previous method, certifying the accuracy of the optimization process.

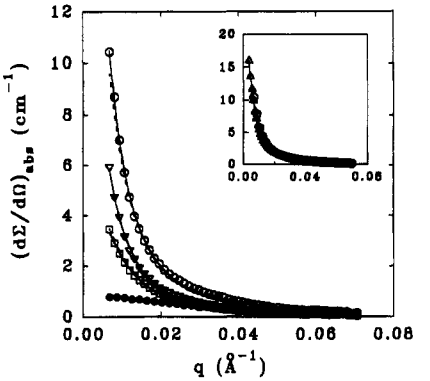


**Figure 2.** Absolute total scattering cross sections of hydrogenated Na-neutralized carboxy-telechelic polystyrene ionomer i-17 in toluene at 25 °C for different polymer concentrations: (○) 1.45, (▽) 1.02, and (□) 0.735 g/dL. Scattering data from the corresponding ester form, e-17, are also shown for comparison: (●) e-17, 1.45 g/dL. The lines represent the fit of the data according to the de Gennes model as described in the text using as a single-chain scattering function (—) the Debye model and (– –) the wormlike chain model. As can be seen, the two single-chain scattering models give almost identical fits. In the inset scattering intensity data of the ionomer at 1.45 g/dL concentration are shown obtained (○) in the $q$ regime as in the main figure and (△) in a lower $q$ regime by altering the system configuration as discussed in the Experimental Section.

**Table 4. Optimized Contrast Factor from the SANS Modeling Analysis and Fractal Dimension of the Telechelic Ionomer Solutions for the Concentrations and Ionic Levels Studied**

| material | $c$ (g/dL) | $K$ ($10^{-3}$ mol·cm$^{-4}$) | $D$ |
|---|---|---|---|
| i-17 | 1.45 | 2.870 | 1.76 |
| | 1.02 | 2.826 | 1.78 |
| | 0.74 | 2.727 | 1.76 |
| i-6 | 2.37 | 2.830 | 1.82 |
| | 1.78 | 2.897 | 1.74 |
| | 1.04 | 2.920 | 1.74 |
| | 0.48 | 2.885 | 1.73 |

The absolute scattering intensity data of the i-17 and i-6 ionomers as a function of concentration are shown in Figures 2 and 3, respectively. A strong upturn of the scattering curves at low $q$ is immediately apparent. This upturn is evident in both ionomer systems and becomes stronger as polymer concentration increases. This upturn is characteristic of the ionomer solutions, as is evidenced from the comparison of the scattering patterns of the ionomers with the corresponding ester forms in Figures 2 and 3. The ester forms, measured under the same experimental conditions as the ionomers, do not show the upturn and have the features expected from nonionic polymer solutions. A comparison between the SANS data of the two ionomers shows that at the same concentration a stronger upturn is observed for the lower ionic content ionomer. This should be compared to the larger solution viscosity that this system exhibits as shown in Figure 1. These data suggest that

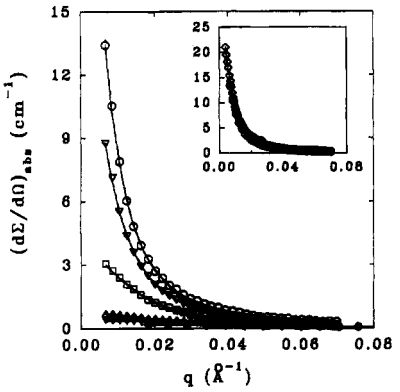


**Figure 3.** Absolute total scattering cross sections of hydrogenated Na-neutralized carboxy-telechelic polystyrene ionomer i-6 in toluene at 25 °C for different polymer concentrations: (○) 2.365, (▽) 1.78, (□) 1.04, and (△) 0.48 g/dL. Scattering data from the corresponding ester form, e-6, are also shown for comparison: (▼) 1.78 and (■) 1.04 g/dL. The solid lines represent the fit of the data according to the de Gennes model as described in the text using as a single-chain scattering function the wormlike chain model. In the inset scattering intensity data of the ionomer at 2.365 g/dL concentration are shown obtained (○) in the $q$ regime as in the main figure and (◇) in a lower $q$ regime by altering the system configuration as discussed in the Experimental Section.

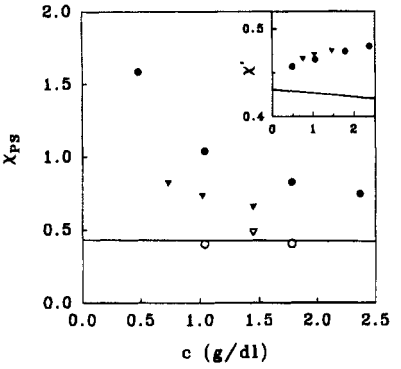


**Figure 4.** Concentration dependence of the Flory–Huggins interaction parameter of the telechelic ionomer solutions in toluene at 25 °C. In the main figure the $\chi_{PS}$ parameter that is predicted from the fitting of the absolute scattering data to the de Gennes model is shown for the ionomers (●) i-6 and (▼) i-17 and the ester forms (○) e-6 and (▽) e-17. The solid line corresponds to the expected concentration dependence of polystyrene/toluene solutions at 25 °C as described in the text. In the inset the concentration dependence of the $\chi'$ interaction parameter that is evaluated from the second virial coefficient of the ionomer solutions, $A_2$, is shown; in this figure the symbols and lines have the same representation as in the main figure.

the scattering upturn observed in the ionomer solutions should be attributed to the ionic association and that the contribution of the intermolecular scattering term, as described by eq 8, in the total scattering function is very important in these solutions. The features observed in the scattering curves of the telechelic ionomer solutions are similar to those observed from SANS experiments on randomly sulfonated polystyrene ionomer solutions in tetrahydrofuran,[8] indicating similar structural characteristics in solution between these ionomer systems although the number and position of the ionic groups along the polymer chain is different. The de Gennes model fit to the data is presented as solid lines in Figures 2 and 3. As can be observed, the de Gennes model successfully fits the ionomer scattering data over the whole $q$ regime at all concentrations and ionic levels studied. The quality of the model fit to the data is more clearly shown in the insets of Figures 2 and 3. In these insets the scattering patterns of the highest concentration studied for each ionomer system are selectively presented and the scattering data are combined with SANS data obtained using a different experimental configuration that enabled access to a lower $q$ regime. Modeling of the two sets of the data resulted in the same values of the fitting parameters which shows the reliability of the de Gennes model to fit an extended $q$-range regime. The data reveal a monotonous increase of the scattering intensity at lower $q$. As there is no evidence of a scattering peak, this result indicates that over the concentration regime studied the aggregates are arranged randomly in solution rather than in an ordered organization.

The de Gennes model predictions of the Flory–Huggins interaction parameter for the ionomer solutions are shown in Figure 4. The ionomer solution interaction parameter shows a quite surprising behavior. For all ionic levels studied, $\chi_{PS}$ is observed to have a strong concentration dependence below 1.5 g/dL. Interestingly, $\chi_{PS}$ is observed to increase with decreasing concentration, which is a result contrary to our expectations, since an increase in $\chi_{PS}$ is related to poorer solvent conditions or in the case of associating solutions to stronger association. Comparison of $\chi_{PS}$ between the esters and the corresponding ionomers as shown in Figure 4 indicates an increased value of $\chi_{PS}$ for the ionomers, as would be expected. From these results it should also be noted that at the same polymer concentration $\chi_{PS}$ is lower for the lower ionic level ionomer solution. Despite the first introduction of $\chi_{PS}$ by Flory as a constant thermodynamic parameter, experimental determination of this parameter in several polymer binary mixtures has shown that, in general, $\chi_{PS}$ is dependent on polymer composition.[67] In this case it has been shown that the exact value of $\chi_{PS}$ depends on the experimental technique applied for its determination.[68] It should be noted that the criterion for a good polymer/solvent system, that $\chi$ is less than 0.5, as well as the direct relationship between $\chi$ and the second virial coefficient, refers to the $\chi$ parameter determined from the excess chemical potential of the solvent, $\chi_{\mu 1}$, at the zero polymer concentration limit. Solutions of polystyrene in toluene at 25 °C have shown a slight decrease of $\chi$ with increasing polymer volume fraction,[69-71] however, data are limited in the very low concentration regime, where it has been observed that $\chi$ also depends on molecular weight. For this system it has been suggested[71] that the concentration dependence of $\chi_{\mu 1}$ is described by: $\chi_{\mu 1} = 0.431 - 0.311\phi_1 - 0.036\phi_1^2$. It can be calculated that the value of $\chi$ determined from scattering experiments, $\chi_{sc}$, will be $\chi_{sc} = 1/(2\phi_1)d(\phi_1^2\chi_{\mu 1})/d\phi_1 = 0.431 - 0.4665\phi_1 - 0.072\phi_1^2$. The concentration dependence of $\chi_{sc}$ is plotted as a solid line in Figure 4 in the concentration regime of interest. As can be observed, this is in good agreement with the FH interaction parameters that have been predicted for the telechelic esters from the de Gennes model fitting.

**C. Molecular Description of the Association Phenomenon.** In dilute polymer solutions information on the molecular parameters as well as the virial coefficients is obtained from a Zimm plot of scattering data in the low-$q$ regime, according to which:

$$\frac{K_N c}{\varrho_1^2 (d\Sigma/d\Omega)_{coh}(q)} = \frac{1}{M_w}\left(1 + \frac{q^2 R_g^2}{3}\right) + 2A_2 c + 3A_3 c^2 + \ldots \quad (10)$$

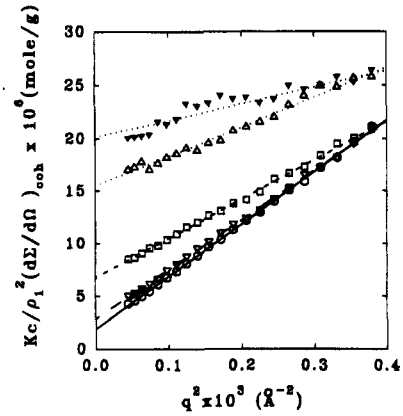


**Figure 5.** Zimm plot of the inverse of the absolute coherent scattering intensity data of the i-6 ionomer system, determined after subtraction of the best fit incoherent scattering intensity according to the de Gennes model from the experimentally measured data versus $q^2$. The symbols are the same as those used in Figure 3. The lines through the data indicate linear regression of the corresponding concentration solutions. Note that the data from the ester have been scaled by a factor of $^1/_7$ from its true value so that a comparison can be made between the ionomer and the ester behavior.

where $R_g^2$ is the $z$-average square radius of gyration ($R_g^2 \equiv \langle R_g^2 \rangle_z$) of the scattering particles. For these solutions, extrapolation to zero concentration and scattering angle is sufficient to determine the molecular parameters of the system. In associating solutions, however, such as low-polarity ionomer solutions, the structure of the solution changes with polymer concentration; therefore, determination of the molecular parameters is not a trivial problem. A parameter that is usually used to obtain information on the association process is the apparent weight-average molecular weight, $(M_w)_{app}$, that is directly attained from the experimental data. This is defined from eq 10 at zero scattering angle as:[72]

$$\frac{1}{(M_w)_{app}(c)} \equiv \frac{K_N c}{\varrho_1^2 (d\Sigma/d\Omega)_{coh,q=0}} = \frac{1}{M_w(c)} + 2A_2(c)\, c + 3A_3(c)\, c^2 + \ldots \quad (11)$$

in analogy to eq 4 for light scattering. The complication that arises in associating polymer systems is that the true molecular weight of the system, $M_w(c)$, as well as the thermodynamic interactions as described by the virial coefficients are concentration dependent. Determination of the $z$-average radius of gyration from a Zimm plot will provide an apparent radius of gyration, $\langle R_g^2 \rangle_{z,app}$, that is related to the true $\langle R_g^2 \rangle_z$ as:

$$\langle R_g^2 \rangle_{z,app} = \langle R_g^2 \rangle_z \frac{(M_w)_{app}}{M_w} \quad (12)$$

By definition, the apparent molecular parameters are an average over all particles as well as over all existing interactions in solution and therefore provide a first evaluation of the true molecular parameters of the system.

For the telechelic ionomer solutions a plot of the inverse scattering intensity versus $q^2$ was linear in the low-$q$ regime, from which evaluation of the apparent molecular parameters of the system was possible. An example of an "equivalent" Zimm plot for the i-6 ionomer and the corresponding ester is shown in Figure 5. The absolute coherent cross sections were obtained after subtraction of the total scattering intensity data from the best fit incoherent scattering obtained from the SANS modeling. A decrease in polymer concentration results in an increase of the intercept of the plot at zero $q$ with a simultaneous decrease of the slope, both approaching the magnitudes of the ester. Similar features were observed for the i-17 ionomer system. These trends provide qualitative evidence that both the apparent average molecular weight and radius of the particles in solution increase with increasing polymer concentration. It is well-known that the validity of the Zimm plot holds for dilute polymer solutions in the low-$q$ regime, where $qR_g < 1$. While the first condition is satisfied for the experimental measurements presented in this paper, for the highest ionomer concentrations studied Zimm plots were applied for $qR_g < 4$. Although it has been shown that for $qR_g > 1$ corrections should be applied in the evaluation of a Zimm plot,[73] the magnitude of these corrections depends on the structure of the polymer solution,[73] and they significantly decrease with increasing polydispersity.[74] While the ionomers are nearly monodisperse, it is expected that the polydispersity of the associating particles in solution will be high, and their structure in solution will be quite different from a probable single-chain structure. Therefore, in the analysis of the apparent molecular parameters of the ionomer solutions, no corrections were applied in the Zimm plots. In addition, we believe that the determination of these parameters from a Zimm plot analysis at the low-$q$ regime is more accurate than that from applying a hypothetical structure factor over the whole $q$ regime, since the formulation of the Zimm plot is independent of the structure and shape of the scattering particles in solution.

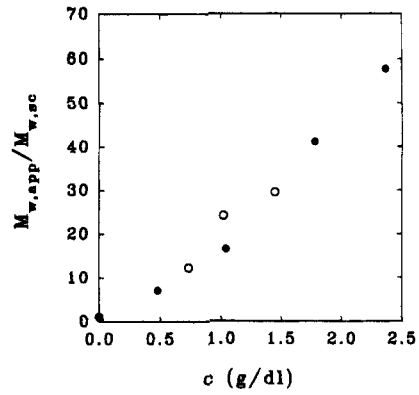


**Figure 6.** Apparent extent of association, defined as the ratio of the apparent weight-average molecular of the associating particles at a specific concentration to the single-chain weight-average molecular weight, versus polymer concentration for the carboxy-telechelic polystyrene ionomers in toluene: (○) i-17 and (●) i-6.

The apparent molecular weight and radius of gyration of the ionomer solutions obtained from this analysis are presented in Figures 6 and 7. From these figures it can be observed that the molecular weight of the particles in solution increases with increasing polymer concentration. The extent of association, defined as the ratio of the particle molecular weight to the single-chain molecular weight, is seen to increase as much as 70 times within a small concentration range of less than 2.5%, indicating how sensitive the association is upon concentration for these solutions. This should be compared with an extent of association of only 10 in the same concentration regime of a 4.2 mol % sodium-neutralized randomly sulfonated polystyrene ionomer.[8]

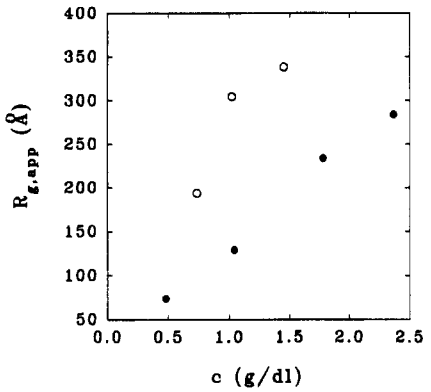


**Figure 7.** Growth of the associating telechelic ionomers in solution as a function of polymer concentration: (○) i-17 and (●) i-6.

This observation is in agreement with the stronger association expected for a similar ionic level telechelic ionomer that eventually leads to gelation compared to a random copolymer ionomer where a gelation transition has not been observed. From the concentration dependence of the apparent molecular weight of the i-6 system the molecular weight of the associating particles is shown to continue increasing with polymer concentration. An unexpected result is that the apparent extent of association appears to be independent of the ionic content at a given polymer concentration. This indicates that, although the associating particles have a different molecular weight due to the different polymer molecular weights, the average number of chains involved in a multimer is the same. The results of another SANS study on similar systems suggested that the multimerization process, as exemplified by the concentration dependence of $M_{w,app}$, is different for different polymer molecular weights.[26] This study suggested that low molecular weight telechelics follow a closed type of association, while higher molecular weight telechelics follow an open association process. However, none of these models could fit the data exactly. In addition, the determination of the $M_{w,app}$ was performed by using the Debye model to describe the scattering from the multimers, which neglects all intermolecular interactions. As will be shown later, analysis of our SANS data at the high-$q$ regime, as well as previous dynamic light scattering studies,[22] suggests that even for the low molecular weight telechelic ionomer system the aggregates formed are of high polydispersity and their molecular weight is concentration dependent.

During the association process, the associating particles also grow in size as shown in Figure 7. The change in particle size is not as large as that observed in molecular weight, and, in addition, the concentration dependence of the apparent radius of gyration appears to be concave down, opposite to the behavior observed for the apparent molecular weight. Also depending on the ionic level, the concentration dependence of the particle size is observed to be different. At all concentrations $R_{g,app}$ is larger for the higher molecular weight ionomer. The stronger increase in viscosity observed as the ionic content decreases in halato-telechelic ionomer solutions is therefore explained in terms of the prepolymer chain length rather than the ionic level. The larger molecular weight of the lower ionic content ionomer leads to the formation of associating particles with the same number of chains but of higher molecular weight and size that are in turn responsible for the larger increase in the solution viscosity.

**D. Supramolecular Structure and True Molecular Parameters of the Association Phenomenon.** In order to determine the true molecular parameters in associating systems, two methods are usually followed in the literature. The first is to assume a physical model that describes the equilibria between multimers of various sizes in solution. In this case the association process can be identified from the concentration dependence of the apparent molecular weight. Such an analysis has been performed in scattering experiments of a 1.39 mol % Na-sulfonated random copolymer polystyrene ionomer in xylene.[11,12] The data were interpreted to follow the open association model, according to which multiple equilibria between unimers and multimers of all sizes take place. However, for such an analysis analytical solutions are available only for two extreme multimerization processes, while identification of the association process requires experimental data obtained over a wide concentration regime.[72]

In this study we shall follow the second method that has been proposed to interpret static light scattering experiments from associating solutions and which takes into account the supramolecular structure of the solutions that resembles the architectures of randomly branched or covalently cross-linked macromolecules.[65,75-79] This method utilizes data that are obtained at the large-$q$ regime which are usually accessible only by SANS experiments. If the ionic association observed in ionomer solutions, as any association phenomenon, is considered as a phenomenon of connectivity, the multimers can be described as fractals, objects that exhibit correlations in the $D$-dimensional space, where $D$ is lower than 3.[80] The weight-average molecular weight of the associating particle is related to the $z$-average radius of gyration of the particle as:

$$M_w \propto R_g^D \tag{13}$$

In all polymer systems studied so far in both good and poor solvents, $A_2$ is a slowly decreasing function of polymer molecular weight.[81] For a relatively narrow range of molecular weights with $\delta$ in the $A_2 \propto M_w^{-\delta}$ range 0.2−0.3. For associating systems, if the molecular weight is large enough, an analogous scaling behavior is observed:[56]

$$A_2(c)\, M_w(c) = K_A M_w^{\alpha'}(c) \tag{14}$$

From eqs 11 and 14, and considering only terms up to the second virial coefficient due to the low-concentration regime studied, the apparent molecular weight can be described as:

$$\frac{1}{(M_w)_{app}(c)} = \frac{1}{M_w(c)}[1 + 2(K_A M_w^{\alpha'}(c))c] \tag{15}$$

The true molecular weight of the system can thus be directly determined from eq 15 once the parameters $\alpha'$ and $K_A$ are known.

The scaling exponent $\alpha'$ depends on the macromolecular architecture and is related to the fractal dimension, $D$, as $\alpha' = (3/D) - 1$. A direct way of evaluating $D$ is from the slope of a double-logarithmic plot of $(d\Sigma/d\Omega)(q)$ versus $q$ which is known to be linear in the intermediate-$q$ regime where $qR_g > 1$. In this range:[82]

$$(d\Sigma/d\Omega)_{coh}(q)/c \propto q^{-D}; \quad qR_g > 1 \tag{16}$$

Double-logarithmic plots of the coherent scattering intensity for the two ionomer systems studied are presented in Figures 8 and 9. The logarithmic plots of

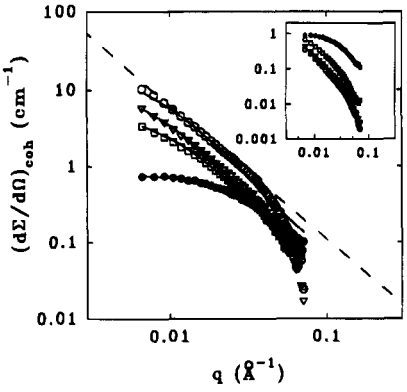


**Figure 8.** Double-logarithmic plots of the coherent scattering intensity of the i-17 ionomer solution at different polymer concentrations and comparison with the ester form. The symbols are the same as in Figure 2. The solid lines are the fit of the data to the de Gennes model. The broken line is from a linear regression of the data at 1.45 g/dL in the regime $4 < qR_g < 10$. The inset of this figure represents the scattering data scaled to the zero $q$ coherent scattering intensity.

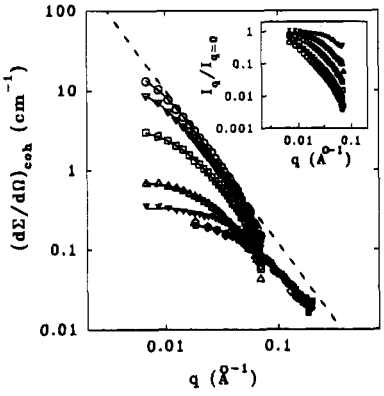


**Figure 9.** Double-logarithmic plots of the coherent scattering intensity of the i-6 ionomer solution at different polymer concentrations and comparison with the ester forms. The symbols are the same as in Figure 3. The solid lines are the fit of the data to the de Gennes model. The lower scattering curves of the ester were evaluated at a sample-to-detector distance of 3 m, a detector center offset of −15 cm, and a neutron wavelength of 6 Å that resulted in a larger $q$ range of 0.0153−0.1909 Å$^{-1}$. The broken line is from a linear regression of the data at 2.365 g/dL in the regime $4 < qR_g < 10$. The inset of this figure represents the scattering data scaled to the zero $q$ coherent scattering intensity.

the ionomers compared with those obtained from the esters exhibit features that are characteristic of network-type systems.[83] The ester forms show a typical plateau in the low-$q$ regime with a linear decrease at higher $q$. As the extent of association in the ionomer solutions proceeds, the scattering intensity increases and is completely dominated by clusters for which $qR_g > 1$, which results in straight lines in the logarithmic plots. At the same polymer concentration, a much lower $q$ range is required for the ionomer solutions to achieve a plateau value compared to the esters, as can be observed from the insets of Figures 8 and 9, where the scattering data have been scaled with respect to the zero scattering intensity. At higher $q$ the scattering intensity of the ionomer drops more abruptly than the ester form. It should be noted that some discrepancies are observed in the fitting of the de Gennes model in the log scale for the i-17 ionomer in the high-$q$ regime, while there are very small deviations in the linear scale. In this representation the fitting of the model for the i-6 ionomer and the esters is very good. From the slopes of the logarithmic plots the values of the fractal dimen-

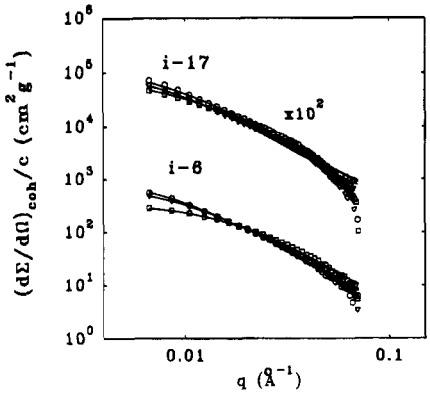


**Figure 10.** Double-logarithmic plots of the scattering intensity versus scattering vector of both ionomer systems i-6 and i-17 scaled with regard to the polymer concentration. The symbols for each ionic system that correspond to different concentrations are the same as those in Figures 8 and 9. The scattering data of the i-17 system have been scaled by a factor of 100 for clarity.

sions were determined considering data in the regime $4 < qR_g < 10$. These results are given in Table 4. As can be observed, the fractal dimension is independent of concentration and is the same within experimental error for both ionic contents examined. This is evidenced in Figure 10 where the scattering intensity has been scaled with respect to concentration. The large $q$ tail of the scattering data is the same for all concentrations and ionic levels studied, while deviations are apparent in the low-$q$ regime because of the different degrees of association exhibited at the different concentration levels. The average value of $D$ is 1.76, which leads to a value of $\alpha$ of 0.71.

$D$ has been observed to depend on the polydispersity as well as the physical state of the system.[82] The fractal dimension has been observed to assume values of 2.0 for monodisperse clusters in solution and 1.60 for polydisperse swollen clusters and can attain values up to 3.0 for more condensed structures. Comparing our result with literature data suggests that the associating particles in the telechelic ionomer solutions form a random type of association with an open rather than a condensed structure. The rather low value of the fractal dimension could be indicative of a high polydispersity in the system. It should be noted that $D$ also depends on the method of gel preparation,[84] and it has been shown to attain a value of 1.75 in a system of monofunctional and multifunctional monomers that can interreact,[85] which is similar to our case. The observed value of fractal dimension is close to the value predicted for a diffusion-limited cluster aggregation (1.8), in contrast to a reaction-limited cluster aggregation (2.1), that is characterized by a rapid aggregation and therefore the existence of large clusters in solution.[86] The observed picture of the supramolecular structure of the ionomer solutions is in agreement with the results drawn from combined SANS/dynamic light scattering experiments on the i-6 ionomer system.[22] These studies showed that the structural parameter $\rho$, defined as the ratio of the $z$-average radius of gyration to the hydrodynamic radius, attains a rather large value for the ionomer solutions, which is suggestive of a high polydispersity of the multimers and the packing of the single chains into extended clusters. Further, our result is closer to the percolation limit predicted for diluted polymer systems (1.60) compared to the Flory classical prediction (1.0).[87] The $D$ value of 1.76 should be compared to an exponent of 1.68 that has been observed

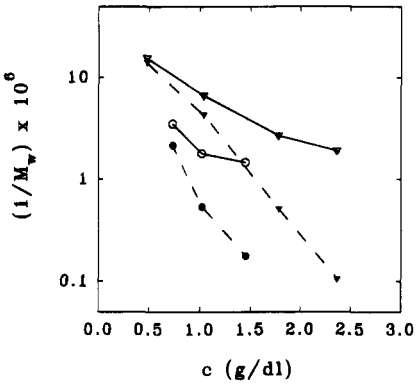


**Figure 11.** Variation of the true molecular weight of the associating particles with concentration. For comparison the corresponding apparent molecular weights are also shown. i-17: (○) $(M_w)_{app}$, (●) $(M_w)_{true}$. i-6: (▽) $(M_w)_{app}$, (▼) $(M_w)_{true}$. The lines shown are simply drawn through the symbols to show the trend of the concentration dependence of the molecular weight of the ionomer solutions. The solid lines correspond to the apparent molecular weights, $(M_w)_{app}$, while the broken lines correspond to the true molecular weights, $(M_w)_{true}$.

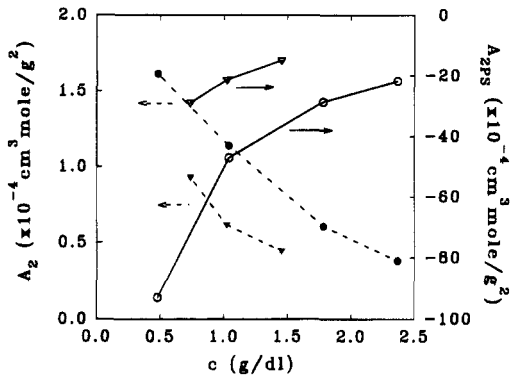


**Figure 12.** Effect of ionic association on the second virial coefficient of the ionomer solutions. The left axis and filled symbols correspond to $A_2$ evaluated from the Zimm plot analysis of the scattering data: (●) i-6 and (▼) i-17. The right axis and open symbols correspond to $A_{2PS}$ that is related to the $\chi_{PS}$ FH interaction parameter from the modeling analysis: (○) i-6 and (▽) i-17. The lines shown are simply drawn through the symbols for clarity. The solid lines correspond to $A_{2PS}$, while the broken lines correspond to $A_2$.

to describe the molecular weight–radius of gyration relationship of linear polystyrene in toluene solutions in the high molecular weight region ($M > 10^5$)[39] which supports the observation that randomly branched polymers display a similar behavior to that of flexible linear chains.

Setting $K_A$ to $4.362 \times 10^{-3}$, the concentration dependence of the true molecular weight is shown in Figure 11. The reason behind choosing this value for $K_A$ will be discussed later. As it can be seen, $1/M_{w,true}$ approaches zero more rapidly than its apparent value for both ionic systems. Comparison between the two ionic levels studied reveals that the divergence in the molecular weight occurs at a much lower concentration for the lower ionic content system. The concentration at which $1/M_w(c) = 0$ leads to the gelation concentration, $c_{gel}$, which provides another means, besides viscosity measurements, for the determination of this parameter in ionomer solutions. These results show very good agreement with the gelation concentration expected from the viscometric measurements shown in Figure 1.

**E. Thermodynamics of Ionomer Solutions.** Evaluation of the thermodynamic interactions in associating polymer solutions, as exemplified by the second virial coefficient, is still an open question. By definition, $A_2$ is the proportionality constant of the first term in the power series in concentration of the osmotic pressure and describes the intramolecular interactions of a polymer chain in a solvent due to the excluded-volume interactions, molecule size, and shape. In ionomer solutions, ionic interactions exist that affect both the inter- and intramolecular interactions. Theoretical analyses of ionomer solutions predict that the ionic interactions affect the excluded volume of the polymer chains by an additive contribution, resulting in a dimensionless second virial coefficient $\hat{A}_2$, where[88,89] $\hat{A}_2 = A_2 + f^2A_2'$. $A_2$ is the second virial coefficient of the solution in the absence of associating groups, $f$ is the fraction of ionic groups along the chain, and $A_2'$ is the second virial coefficient due to dipolar interactions, which is always negative due to the attractive ionic interactions. In addition, in associating polymer solutions, the second virial coefficient will include binary interactions within a cluster rather than a chain.

In eq 11, the term that describes the intermolecular interactions is included in the true molecular weight of the system, while the virial coefficient term describes all other interactions. The parameter $K_A$ that is required for the evaluation of $A_2$ in eq 11 is concentration independent. Based upon the similarity that has been observed in the behavior between randomly branched polymers and flexible linear chains, a first approach to this problem is to assume that $A_2$ is the second virial coefficient of the corresponding nonionic polymer solution at large molecular weight. The molecular weight scaling of the second virial coefficient of high molecular weight linear polystyrene solutions in toluene at 25 °C has been evaluated as[39] $A_2 = 4.362 \times 10^{-3}M_w^{-0.203}$ which leads to $K_A = 4.362 \times 10^{-3}$. This result is lower than that expected if $(A_2)_{c=0}$ was considered to be that of the parent polymer solution, in which case $K_A$ would be ~0.0166 for i-6 and 0.0139 for i-17. The similarity in these two values may justify the use of the same $K_A$ for both ionomer systems. The second virial coefficient of the ionomer solutions determined from eq 14 is shown in Figure 12. As observed from this plot, $A_2$ for both ionomer systems studied shows a strong concentration dependence. With increasing polymer concentration, or increasing degree of association, $A_2$ is seen to significantly decrease, indicating that the presence of ionic groups changes the thermodynamic state of the ionomer solutions, with the solvent becoming a poor solvent for the ionomers even though it is a good solvent for the polymer. At all concentrations studied $A_2$ for the ionomers is lower than the corresponding esters. Furthermore, $A_2$ is lower for the lower ionic content ionomer which is expected due to the higher association that has been observed for this system. Previous information on the second virial coefficient of ionomer solutions has mostly been obtained from static light scattering experiments in dilute random copolymer ionomer solutions. In these studies $A_2$ was evaluated from the slope of $1/(M_w)_{app}$ versus concentration and was shown to decrease with increasing ionic content (increasing extent of association) approaching zero,[7] and even assuming negative values for low polymer molecular weights.[90] Although this behavior is similar to that observed in the telechelic ionomer solutions presented in this study, the determination of $A_2$ in the previous studies has been confined mainly to the zero concentration limit. The results from this study show that the ionomer solution thermodynamic interactions are strongly dependent

upon the extent of aggregation. The observed concentration dependence of $A_2$ and $M_w$ of the telechelic ionomer solutions has been seen to follow the same qualitative behavior for different positive values of $K_A$ that have been examined. Studies are under way to determine the exact molecular parameters of the system by probing more dilute polymer concentrations via static light scattering measurements.

Another means of determining the second virial coefficient of the ionomer solutions would be from the Flory–Huggins interaction parameter $\chi$ that has been evaluated from the modeling of the SANS data. However, due to the concentration dependence of all the molecular and thermodynamic parameters of the system, such a calculation is not straightforward, as was also discussed in the previous sections. A discussion is warranted, however, in order to understand the relation between the $\chi_{PS}$ parameter that was evaluated from the modeling analysis and the second virial coefficient evaluated from the Zimm plot. The application of the de Gennes model to the ionomer solutions, according to eq 9, is equivalent to writing the Zimm equation in analogy to eq 5, considering that the molecular weight term corresponds to the single-chain molecular weight. By comparing eqs 9 and 5 at zero $q$, the second virial coefficient, $A_{2PS}$, that is related to $\chi_{PS}$ is:

$$A_{2PS} = \frac{1}{2\varrho_1^2\phi_0 V_0} - \frac{\chi_{PS}}{\varrho_1^2 v_0} \tag{17}$$

$A_{2PS}$ of the ionomer solutions has been included in Figure 12 to facilitate a direct comparison with the second virial coefficient, $A_2$, obtained from the Zimm plot analysis. As seen in this figure, such an evaluation results in large negative virial coefficients for the ionomer solutions which is evidence of the domination of attractive ionic interactions. At larger concentrations, $A_{2PS}$ approaches zero, which is expected with the appearance of a gel transition.

The significant difference that is observed in the behavior between $A_2$ and $A_{2PS}$, as well as the large values that were attained for the $\chi_{PS}$ parameter, can therefore be viewed in terms of the different physical interpretation that these parameters represent. In the evaluation of $\chi_{PS}$, or equivalently $A_{2PS}$, the effect of ionic association on the state of the solution was considered to reside entirely in the terms that describe the interaction parameters. Therefore, the interaction parameters include all the intra- and intermolecular interactions that take place in solution. For associating systems, however, the thermodynamics of the polymer solution has to take into account the free energy of mixing of a solution that consists of multichain aggregates. Application of the Flory–Huggins equation for a multicomponent system would lead to writing the de Gennes model at zero $q$ as:[65,91]

$$\frac{K_N}{[(d\Sigma/d\Omega)_{coh}]_{q\to 0}} = \frac{1}{Z_w\phi_1 V_1} + \frac{1}{\phi_0 V_0} - \frac{2\chi'}{v_0} \tag{18}$$

This is written in exactly the same manner as eq 9, with the only difference being that the first term corresponds to the average over all aggregates existing in solution as noted in the insertion of the weight-average degree of polymerization of the aggregate particles, $Z_w$. The FH interaction parameter that is determined in this case, $\chi'$, describes only the intramolecular interactions within the aggregates and is therefore the one that is directly related to the second virial coefficient that was evaluated previously from the Zimm plot analysis of the SANS data. Comparison of eqs 9 and 18 shows that $\chi'$ is related to $\chi_{PS}$ by a simple additive relation as:

$$\chi_{PS} - \chi' = \frac{v_0 M_0}{2V_1\phi_1}\left(\frac{1}{M_{w,sc}} - \frac{1}{M_{w,true}}\right) \tag{19}$$

The parameter $\chi'$ for the telechelic ionomer solutions is shown in the inset of Figure 4. $\chi'$ is observed to be increasing with concentration, which is the result expected of an association phenomenon. At larger concentrations $\chi'$ is seen to approach the critical value of 0.5. Comparison between $\chi'$ and the FH interaction parameter of the esters suggests that the actual segmental interactions between the monomers and the solvent are affected by the association becoming poorer as the extent of association increases. Although the determination of $\chi'$ relies on knowledge of $M_{w,true}$ as shown in eq 19, its contribution is not significant due to the large values that $M_{w,true}$ attains in the concentration regime studied. In fact, the exact value of $M_{w,true}$ affects the absolute value of $\chi'$ but not its concentration dependence. It is apparent that the presence of ionic association has a significant impact on the thermodynamic interactions of these solutions compared to their nonionic counterparts. A precise evaluation of the interaction parameters in associating solutions from scattering experiments requires theoretical reconsideration in order to fully account for their concentration dependence in the derivation of the scattering equations from the expression of the free energy of the system.

## IV. Conclusions

The molecular mechanism that leads to a strong enhancement in the solution viscosity of sodium-neutralized carboxy-telechelic polystyrene ionomers in toluene is also apparent in the scattering patterns of these solutions as evidenced by a strong upturn in small-angle neutron scattering experiments in the low-$q$ regime. This upturn is characteristic of the ionomer solutions as compared to the corresponding ester forms and is attributed to strong intermolecular interactions that prevail in these solutions. In the dilute concentration regime studied ionic association does not lead to ordered structures in solution. The effect of ionic interactions is quite dramatic on both the molecular and thermodynamic state of the solutions. With increasing concentration the average number of chains associated into an aggregate particle increases several orders of magnitude over a relatively short concentration range. The molecular weight and size of the aggregates is larger for a lower ionic content ionomer which explains the rather unexpected viscometric behavior of telechelic ionomer solutions that show a stronger viscosity enhancement with decreasing ionic level. Quite surprisingly, the apparent extent of association appears to be independent of ionic level over the concentration regime studied, although the two ionomer systems differ by almost a factor of 2 in polymer chain length. The existence of a gelation transition is evidenced by a divergence of the true molecular weight of the particles at higher concentrations. The scattering intensity of the ionomer solutions can be described by a scaling law in the $q$ dimension that is expected for systems that show connectivity. The statistics of the association process are closer to the predictions expected from the percolation approach rather than classical thermodynamic

arguments. The fractal dimension of the aggregates for both ionic levels studied has a value of 1.76 which suggests that the supramolecular structure of the telechelic ionomer solutions is dominated by polydisperse clusters that prefer an extended rather than a condensed configuration.

The effect of ionic association on the polymer–solvent interaction was most dramatically demonstrated by application of the de Gennes model to the ionomers which considers the thermodynamics between single polymer chains and solvent molecules. While the model analysis provided reasonable results for the telechelic esters, it revealed a strong concentration dependence of the Flory–Huggins interaction parameter for the ionomer solutions. Quite unexpectedly, $\chi_{PS}$ for the ionomer solutions showed an increase with decreasing concentration for both ionic systems studied, which is contrary to our expectations for association. However, in comparison between the ionomers and the esters the expected increase of $\chi_{PS}$ on going from the ester to the ionomer occurs. Evaluation of the interactions in the ionomer solutions reveals that the thermodynamic state of the polymer clusters changes with respect to the single polymer chains. The polymer–solvent interactions in the ionomer solutions are strongly dependent on the degree of association and become poorer with increasing concentration and decreasing ionic level.

**Acknowledgment.** We especially thank Dr. Boualem Hammouda at NIST for his extensive assistance, interest, and valuable discussions during the neutron scattering experiments. We also thank J. Zhang for helping in the synthesis of the materials and Brian P. Grady for helping with the SANS experiments. We acknowledge the National Institute of Standards and Technology (NIST) for providing the beam time and its facilities for making this study possible. R.J. is grateful to the "Services Fédéraux des Affaires Scientifiques, Techniques et Culturelles" for financial support. This work has been supported by the Department of Energy through Grant DE-FG02-88ER45370.

## References and Notes

(1) Eisenberg, A. *Macromolecules* **1970**, *3*, 147.
(2) Lantman, C. W.; MacKnight, W. J.; Lundberg, R. D. *Annu. Rev. Mater. Sci.* **1989**, *19*, 295.
(3) Tant, M. R.; Wilkes, G. R. *J. Macromol. Sci., Rev. Macromol. Chem. Phys.* **1988**, *C28*, 1.
(4) Lundberg, R. D.; Phillips, R. R. *J. Polym. Sci., Polym. Phys. Ed.* **1982**, *20*, 1143.
(5) Fitzgerald, J. J.; Weiss, R. A. *J. Macromol. Sci., Rev. Macromol. Chem. Phys.* **1988**, *C28*, 99.
(6) Lundberg, R. D. In *Structure and Properties of Ionomers*; Pineri, M., Eisenberg, A., Eds.; NATO ASI Series C198; D. Reidel: Holland, 1987; p 361.
(7) Lantman, C. W.; MacKnight, W. J.; Peiffer, D. G.; Sinha, S. K.; Lundberg, R. D. *Macromolecules* **1987**, *20*, 1096.
(8) Lantman, C. W.; MacKnight, W. J.; Sinha, S. K.; Peiffer, D. G.; Lundberg, R. D.; Wignall, G. D. *Macromolecules* **1988**, *21*, 1339.
(9) Lantman, C. W.; MacKnight, W. J.; Higgins, J. S.; Peiffer, D. G.; Sinha, S. K.; Lundberg, R. D. In *Multiphase Polymers: Blends and Ionomers*; Utracki, L. A., Weiss, R. A., Eds.; ACS Symposium Series 395; American Chemical Society: Washington, DC, 1989; p 446.
(10) Gabrys, B.; Higgins, J. S.; Lantman, C. W.; MacKnight, W. J.; Pedley, A. M.; Peiffer, D. G.; Rennie, A. R. *Macromolecules* **1989**, *22*, 3746.
(11) Pedley, A. M.; Higgins, J. S.; Peiffer, D. G.; Burchard, W. *Macromolecules* **1990**, *23*, 1434.
(12) Pedley, A. M.; Higgins, J. S.; Peiffer, D. G.; Rennie, A. R. *Macromolecules* **1990**, *23*, 2494.
(13) Bakeev, K. N.; Teraoka, I.; MacKnight, W. J.; Karasz, F. E. *Macromolecules* **1993**, *26*, 1972.
(14) Williams, C. E. In *Contemporary Topics in Polymer Science*; Gulbertson, W. M., Ed.; Plenum: New York, 1989; Vol. 6, p 639.
(15) Broze, G.; Jérôme, R.; Teyssié, Ph. *Macromolecules* **1982**, *15*, 920.
(16) Broze, G.; Jérôme, R.; Teyssié, Ph. *Macromolecules* **1981**, *14*, 224.
(17) Jérôme, R.; Broze, G.; Teyssié, Ph. In *Microdomains in Polymer Solutions*; Duhem, P., Ed.; Plenum: New York, 1985; p 243.
(18) Tant, M. R.; Wilkes, G. L.; Storey, R.; Kennedy, J. P. *Polym. Bull.* **1985**, *13*, 541.
(19) Hara, M.; Wu, J.; Wang, Y.; Jérôme, R.; Granville, M. *Polym. Prepr. (Am. Chem. Soc., Div. Polym. Chem.)* **1989**, *30*, 219.
(20) Hara, M.; Wu, J. L.; Lee, A. H. *Macromolecules* **1988**, *21*, 2214.
(21) Granville, M.; Jérôme, R.; Teyssié, Ph.; De Schryver, F. C. *Macromolecules* **1988**, *21*, 2894.
(22) Karayianni, E.; Cooper, S. L. *Ind. Eng. Chem. Res.* **1994**, *33*, 2492.
(23) Broze, G.; Jérôme, R.; Teyssié, Ph. *Macromolecules* **1982**, *15*, 1300.
(24) Jérôme, R. In *Structure and Properties of Ionomers*; Pineri, M., Eisenberg, A., Eds.; NATO ASI Series C198; D. Reidel: Holland, 1987; p 399.
(25) Grady, B. P.; Karayianni, E.; Goddard, R. J.; Cooper, S. L. *Polym. Mater. Sci. Eng.* **1992**, *67*, 128.
(26) Timbo, A. M.; Higgins, J. S.; Peiffer, D. G.; Maus, C.; Vanhoorne, P.; Jérôme, R. *J. Phys. IV* **1993**, *C8*, 71.
(27) Vanhoorne, P.; Van den Bossche, G.; Fontaine, F.; Sobry, R.; Jérôme, R.; Stamm, M. *Macromolecules* **1994**, *27*, 838.
(28) Jérôme, R. In *Telechelic Polymers: Synthesis and Applications*; Goethals, E. J., Ed.; CRC Press: Boca Raton, FL, 1989, Chapter 11.
(29) Register, R. A.; Cooper, S. L.; Thiyagarajan, P.; Chacrapani, S.; Jérôme, R. *Macromolecules* **1990**, *23*, 2978.
(30) Wolff, C. *Eur. Polym. J.* **1977**, *13*, 739.
(31) Kulicke, W.-M.; Kniewske, R.; Klein, J. *Prog. Polym. Sci.* **1982**, *8*, 373.
(32) Dondos, A. *Makromol. Chem., Macromol. Symp.* **1992**, *62*, 129.
(33) Han, C. C. *Polymer* **1979**, *20*, 1083.
(34) McCrackin, F. L. *Polymer* **1987**, *28*, 1847.
(35) Kniewske, R.; Kulicke, W. M. *Makromol. Chem.* **1983**, *184*, 2173.
(36) Hager, B. L.; Berry, G. C.; Tsai, H.-H. *J. Polym. Sci., Polym. Phys. Ed.* **1987**, *25*, 387.
(37) Bender, T. M.; Lewis, R. J.; Pecora, R. *Macromolecules* **1986**, *19*, 244.
(38) Johnson, B. L.; Smith, J. In *Light Scattering from Polymer Solutions*; Hugglin, M. B., Ed.; Academic Press: New York, 1971; Chapter 2.
(39) Huber, K.; Bantle, S.; Lutz, P.; Burchard, W. *Macromolecules* **1985**, *18*, 1461.
(40) Hadjichristidis, N. J.; Fetters, L. J. *J. Polym. Sci., Polym. Phys. Ed.* **1982**, *20*, 2163.
(41) Chau, T. C.; Rudin, A. *Polymer* **1974**, *15*, 593.
(42) Barrall, E. M., II; Cantow, M. J. R.; Johnson, J. F. *J. Appl. Polym. Sci.* **1968**, *12*, 1373.
(43) Sato, T.; Norisuye, T.; Fujita, H. *J. Polym. Sci., Polym. Phys. Ed.* **1987**, *25*, 1.
(44) *NIST Progress Report 1992*; NIST: Gaithersburg, MD, 1993.
(45) Kostorz, G.; Lovesey, S. W. In *Treatise on Materials Science and Technology*; Academic Press: New York, 1979; Vol. 15, p 1.
(46) Higgins, J. S.; Maconnachie, A. In *Polymer Solutions*; Forsman, W. C., Ed.; Plenum: New York, 1986; Chapter 4.
(47) Higgins, J. S.; Maconnachie, A. In *Neutron Scattering*; Price, D. L., Skold, K., Eds.; Academic Press: New York, 1984; Chapter 22.
(48) (a) Scholte, Th. G. *J. Polym. Sci., Polym. Phys.* **1972**, *10*, 519. (b) Sarazin, D.; Francois, J. *Polymer* **1978**, *19*, 694. (c) Rawiso, M.; Duplessix, R.; Picot, C. *Macromolecules* **1987**, *20*, 630.
(49) Perry, R. H.; Green, D. *Perry's Chemical Engineers' Handbook*, 6th ed.; McGraw-Hill: New York, 1984.
(50) Richards, R. W. *Compr. Polym. Sci.* **1989**, *1*, Chapter 6.
(51) Higgins, J. S. In *Treatise on Materials Science and Technology*; Academic Press: New York, 1979; Vol. 15, p 381.
(52) Moore, W. R. In *Progress in Polymer Science*; Jenkins, A. D., Ed.; Pergamon Press: Oxford, 1967; Vol. 1.
(53) Wolff, C.; Silberberg, A.; Priel, Z.; Layec-Raphalen, M. N. *Polymer* **1979**, *20*, 281.
(54) Dort, I. *Polymer* **1988**, *29*, 490.
(55) Higgins, J. S.; Stein, R. S. *J. Appl. Crystallogr.* **1978**, *11*, 346.

(56) de Gennes, P.-G. *Scaling Concepts in Polymer Physics*; Cornell University Press: Ithaca, NY, 1979.
(57) Boué, F.; Nierlich, M.; Leibler, L. *Polymer* **1982**, *23*, 29.
(58) Zimm, B. *J. Chem. Phys.* **1948**, *16*, 1093.
(59) Benoit, H.; Benmouna, M. *Macromolecules* **1984**, *17*, 535.
(60) Hammouda, B. *Adv. Polym. Sci.* **1993**, *106*, 88.
(61) Benoit, H.; Benmouna, M. *Polymer* **1984**, *25*, 1059.
(62) Karayianni, E.; Cooper, S. L., manuscript in preparation.
(63) Cotton, J. P.; Decker, D.; Farnoux, B.; Jannink, G.; Ober, R.; Picot, C. *Phys. Rev. Lett.* **1974**, *32*, 1170.
(64) Sharp, P.; Bloomfield, V. A. *Biopolymers* **1968**, *6*, 1201.
(65) Flory, P. J. *Principles of Polymer Chemistry*; Cornell University Press: Ithaca, NY, 1953.
(66) (a) Wignall, G. D.; Bates, F. S. *Makromol. Chem.* **1988**, *15*, 105. (b) Bates, F. S.; Wignall, G. D.; Koehler, W. C. *Phys. Rev. Lett.* **1985**, *55*, 2425.
(67) Flory, P. J. *J. Chem. Soc., Faraday Discuss.* **1970**, *49*, 7.
(68) Sanchez, I. C. *Polymer* **1989**, *30*, 471.
(69) Masegosa, R. M.; Prolongo, M. G.; Horta, A. *Macromolecules* **1986**, *19*, 1478.
(70) Kinugasa, S.; Hayashi, H.; Hamada, F.; Nakajima, A. *Macromolecules* **1985**, *18*, 582.
(71) Brandrup, J.; Immergut, E. H. *Polymer Handbook*; 3rd ed.; John Wiley & Sons: New York, 1989.
(72) Elias, H. G. In *Light Scattering from Polymer Solutions*; Huglin, M. B., Ed.; Academic Press: London, 1972, Chapter 9.
(73) Ullman, R. *J. Polym. Sci., Polym. Lett. Ed.* **1983**, *21*, 521.
(74) Ullman, R. *J. Polym. Sci., Polym. Phys. Ed.* **1985**, *23*, 1477.
(75) Burchard, W. *Makromol. Chem., Macromol. Symp.* **1990**, *39*, 179.
(76) Burchard, W.; Schulz, L.; Auersch, A.; Littke, W. *Polym. Prepr. (Am. Chem. Soc., Div. Polym. Chem.)* **1990**, *31* (2), 131.
(77) Burchard, W.; Lang, P.; Schulz, L.; Coviello, T. *Makromol. Chem., Macromol. Symp.* **1992**, *58*, 21.
(78) Stockmayer, W. H. *J. Chem. Phys.* **1943**, *11*, 45.
(79) Stauffer, D. *Introduction to Percolation Theory*; Taylor and Francis: London and Philadelphia, 1985.
(80) Witten, T. A.; Sander, L. M. *Phys. Rev. B* **1983**, *2*, 5686.
(81) Fujita, H. *Polymer Solutions*; Elsevier: Amsterdam, Holland, 1990.
(82) Bouchaud, E.; Delsanti, M.; Adam, M.; Daoud, M.; Durand, D. *J. Phys. (Paris)* **1986**, *47*, 1273.
(83) Chen, S. H.; Sheu, E. Y.; Kalus, J.; Hoffmann, H. *J. Appl. Crystallogr.* **1988**, *21*, 751.
(84) Adam, M.; Delsanti, M.; Munch, J. P.; Durand, D. *J. Phys. (Paris)* **1987**, *48*, 1809.
(85) Candau, S. J.; Ankrim, M.; Munch, J. P.; Rempp, P.; Hild, G.; Okasha, R. *Physical Optics of Dynamic Phenomena and Processes in Macromolecular Systems*; de Gruyter, W., Ed.; Berlin, New York, 1985.
(86) Klein, R.; Weitz, D. A.; Lin, M. Y.; Lindsay, H. M.; Ball, R. C.; Meakin, P. *Prog. Colloid Polym. Sci.* **1990**, *81*, 161.
(87) Daoud, M.; Family, F.; Jannink, G. *J. Phys. Lett.* **1984**, *45*, L-199.
(88) Joanny, J. F. *Polymer* **1980**, *21*, 71.
(89) Cates, M. E.; Witten, T. A. *Macromolecules* **1986**, *19*, 732.
(90) Hara, M.; Wu, J. L. *Macromolecules* **1988**, *21*, 402.
(91) Stockmayer, W. H. *J. Phys. Chem.* **1992**, *96*, 4084.

MA950025W